

Metal Oxide Surface Additives for Xerographic Toner: Adhesive Forces and Powder Flow

Richard Veregin and Robert Bartha
Xerox Research Centre of Canada
2660 Speakman Drive, Mississauga, Ontario, Canada, L5L 5C3

Abstract

Xerographic toners use submicron metal oxide surface additives to control powder flow. Indeed, oxides have been used to improve flowability or compressibility of cohesive powders for decades, from coffee whitener to aspirin. To date there has been little attempt to understand the mechanism of action of flow aids. In this paper, toner powder cohesion was measured with respect to the primary particle size, hydrophobicity, and hydrogen bonding of the oxide. Cohesion is interpreted in terms Van der Waals, capillary, and hydrogen bonding forces. Flow with oxides is determined by the nano-geometry of contact between oxide particles, determined by the oxide primary particle size. Adhesion forces decrease with decreasing oxide primary particle size and increasing hydrophobicity.

Introduction

This paper studies adhesion of toner with surface oxides (used to control toner flow, charge[1-5] and transfer.[6])

Experimental

Toner flow was measured on a Hosokawa Micron Powder tester, which applies a vibration for 90 s to 2 g of toner on a set of sieves (Figure 1). The % cohesion is:

$$\% \text{ cohesion} = 50 \bullet A + 30 \bullet B + 10 \bullet C \qquad (1)$$

A, B and C are the toner weights left on each screen. Eq 1 applies a weighting factor proportional to screen size.

Table 1 lists the toners used; Table 2 the oxides. Additives were blended at 24 krpm using a coffee mill.

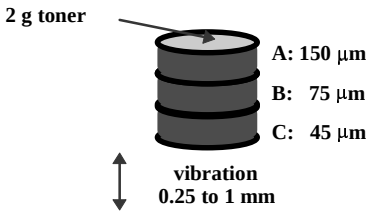

Figure 1. Powder cohesion test setup.

Table 1. Base Toner Particles

Toner ID	Resin ID	Pigment Type	wt%
A1-A3	1	unoxidized CB	6.0
B1-B5	2	cyan	4.0
C	3	none	0
D	3	oxidized carbon black	4.2
E	3	oxidized carbon black	7.2
F	3	unoxidized carbon black	4.7
G	3	unoxidized carbon black	19.3
H	3	magenta	6.0
I	3	cyan	6.0
J1,J2	4	cyan	6.0
K1,K2	5	none	0

Table 2. Flow Additives

Additive	Base Oxide	Treated	Hydro-phobic	H-Bonds
Degussa A380	7 nm silica	none	no	yes
Degussa R812	7 nm silica	HMDS	yes	no
Degussa MOX170	15 nm silica	none	no	yes
Degussa R972	16 nm silica	DMCS	yes	no
Degussa TT600	40 nm silica	none	no	yes
Degussa P25	21 nm TiO_2	none HMDS	no yes[8]	no no
Degussa Al_2O_3	20 nm Al_2O_3	none HMDS	no yes	no no
A*	100 nm *	*	no	no

* Proprietary; HMDS =$((CH_3)_3SiN)_2$;DMCS=$(CH_3)_3SiCl_2$

Results and Discussion

Powder Cohesion Test and Interparticle Forces

The literature is silent except for Carr's assertion[7] that there is a quantitative relationship between adhesive force and Hosokawa cohesion. Toner consists of agglomerated particles. Assume that the ensemble cohesion follows a Gaussian distribution (eq 2 and Figure 2).

$$N_F = \frac{N_0}{\sqrt{2\pi}\ \sigma} \exp\left(\frac{(F - \overline{F})^2}{2\sigma^2}\right) \qquad (2)$$

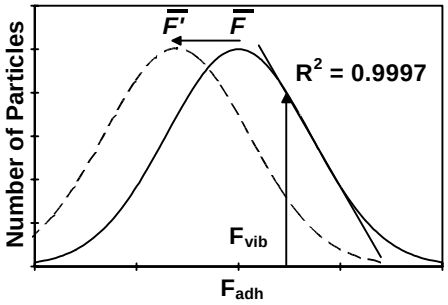

Figure 2. Relationship between Gaussian toner force distribution and Hosokawa powder cohesion test. Two powders of different average interparticle forces are shown.

The screen vibration applies a defined force, F_{vib}, to the toner. If F_{vib} is large enough to break the agglomerates they will go through the screen. If F_{vib} is large enough to separate ≅60% of the particles (but less than ≅90%), as shown in Figure 2 ($\overline{F}$ = average cohesive force), then the number of particles separated will be linearly related to $F_{vib.}$ Similarly, if the average particle cohesive force changes from $\overline{F}$ to $\overline{F}'$ (Figure 2), at constant F_{vib}, then the number of particles that will pass through the screens is linear in $\overline{F}$. Carr[7] has been clever in using different size screens. The smaller screen requires a larger force to pass toner. Even if all the toner passes one screen, the smaller screen below can partition toner in its linear range, extending the measurement range. There are two hidden assumptions. The first is that cohesion is linear in screen size. The second is that the width of the cohesive force distribution is constant. For example, narrowing the distribution results in an apparent lower cohesion for the conditions in Figure 2, even if $\overline{F}$ is unchanged. This too is compensated by different size screens, at least if there is toner on more than one screen (a screen on each side of $\overline{F}$ in Figure 2).

Overall, there is a reason to expect an approximately linear relation between Hosokawa cohesion and interparticle forces, provided that ≅10% to 40% (or 60 to 90%) of toner is on at least one screen. This condition is fulfilled for tests here (excepting those below 2% cohesion).

Surface Coverage of Additives on Toner

Oxide surface coverage was estimated assuming a spherical oxide primary particle of radius *r*, and a spherical toner of radius, *R*. Eq 2 assumes the particles pack in hexagonal close packing. For 100% surface coverage:[9]

$$wt\%\ additive = 100 \bullet \frac{2 \bullet \pi}{\sqrt{3}} \bullet \frac{\rho_a \bullet r}{\rho_t \bullet R} \qquad (3)$$

In fact, oxides are fractal fused aggregates of primary spherical particles, which are not broken down during toner blending. Thus, while primary sizes are often quoted, the aggregate on the toner is larger: 300 to 500 nm. Due to the fractal architecture these particles will not cover all the toner surface expected, as shown in Figure 3.

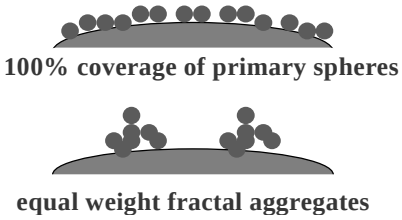

Figure 3. Additives on surface of toner after blending.

Van der Waals Forces

All materials are subject to Van der Waals forces, which depends on instantaneous polarization of electrons in one material due to electromagnetic interaction with electrons in another material, as derived by Lifshitz[10]:

$$F_V = \frac{\hbar \varpi r}{16 \pi L^2} \qquad (4)$$

$\hbar\omega$ (10^{-11} to 10^{-13} ergs) depends on the materials and intervening medium ($\varepsilon_{materials}$, ε_{medium}, $n_{materials}$ and n_{medium}, where *n* = refractive index and ε = dielectric constant), $\hbar$ is Planck's constant, *L* is the Van der Waals contact distance (≅0.5nm), and *r* is the contact radius of the curvature from surface asperities. If there are surface additives then r is the radius of the oxide primaries (not the aggregate).

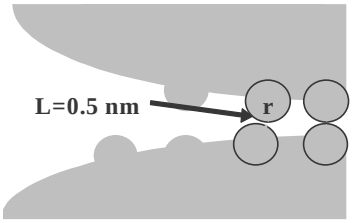

Figure 4. The contact of toner particles at asperities.

Capillary Forces

Water on surfaces creates capillary forces.[11-13] Water is in a pendular state on toner (Figure 5), as there are less than a few monolayers (0.35 nm/monolayer.[13]). The water is insufficient to bridge asperities (which are 50 to 100 nm for bare toner, or 7 to 50 nm with flow aid, as shown later). The water meniscus creates a force:[11-13]

$$F_{capillary} = 2 \pi r \sigma_z (l - L/2) \qquad (5)$$

Here, σ_z is the tensile strength of water (9.8×10^7 dynes/cm^2), and *l* = thickness of the water layer.

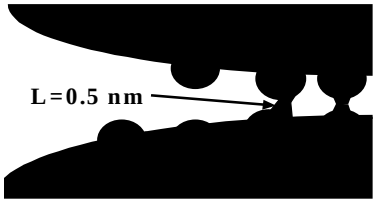

Figure 5. Pendular water between toner asperities.

Hydrogen Bonding

Toner surface groups that form hydrogen bonds will create an interparticle force. Figure 6 shows the contact of two silica primaries of radius *r*. Interparticle H-bonds form between -OH groups within an area, $S_{H\text{-}bond}$, of "radius" *a* from the "contact". Outside this area the water layer separation, *2L* (=H-bond length), is too large for an H-bond, due to surface curvature. Since $a << r$, $S_{H\text{-}bond} = \pi a^2$, $s = r\theta \cong h \cong a$, $\sin\theta \cong \theta$, and $L = h \bullet \sin(\theta/2)$.

$$S_{H\text{-}bond} = \pi a^2 = \pi (r\theta)\,(L/\sin(\theta/2) = 2\pi r L \qquad (6)$$

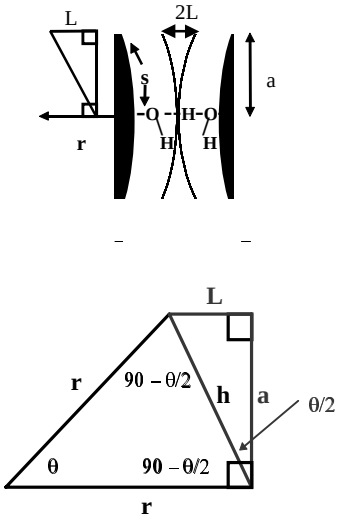

Figure 6. Geometry for interparticle H-bond area in eq 6.

The adhesive force is ($\rho_{H\text{-}bond}$ = surface area density of H-bonds, and $f_{H\text{-}bond}$ = bond strength):

$$F_{H\text{-}Bond} = 2\,\pi L\,\rho_{H\text{-}Bond}\,f_{H\text{-}Bond}\,r \qquad (7)$$

Overall, all of the interparticle forces are linear in the asperity radius: larger asperities result in larger forces.

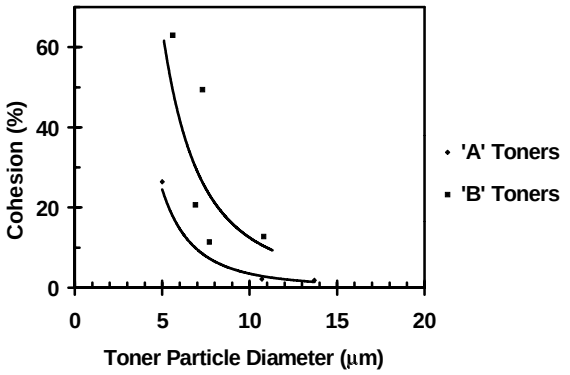

Figure 7. Powder cohesion with toner particle size.

Toner Powder Flow Cohesion Tests

Why do we now worry about flow when early toners had no flow additives? Figure 7 shows one reason, illustrated by two toner series. In each series decreased particle size shows a dramatic cohesion increase. The current trend to small toner increases the need for flow additives.

Figure 8 shows that as the loading of pigment changes there is a linear change in cohesion. For small carbon blacks, less than 60 nm in primary size (black toners), cohesion drops linearly with pigment loading. The smaller the pigment, the larger the effect as a flow aid, as expected from eq 4, 5 and 7. To act in this way, pigment must be on the toner surface, proportional to the bulk concentration. Color pigments are larger than these carbon blacks, and show a linear **increase** in cohesion with loading. Thus, the bare toner asperity size is 60 to 100 nm: smaller pigments are flow aids, larger pigment particles are adhesives.

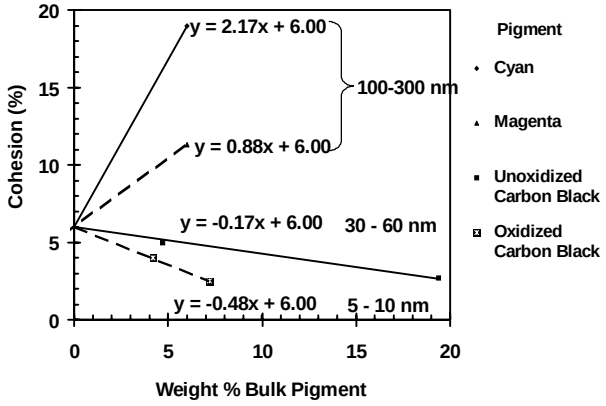

Figure 8. Toner cohesion with pigment type and loading.

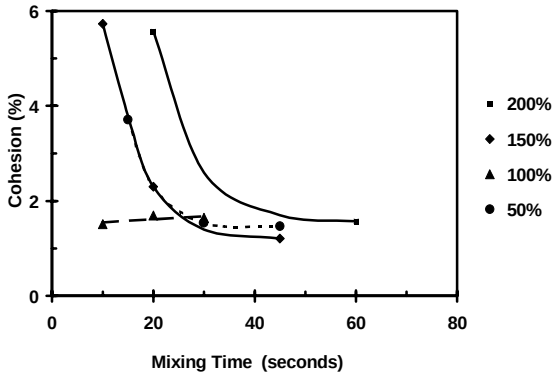

Figure 9. Coffee mill blending of R812 on toner J2

Figure 9 shows toner cohesion with additive blending time for various theoretical coverage's (eq 3). At 50% coverage cohesion drops rapidly, close to the lower limit of the cohesion test (1.5 %). At 100% coverage, cohesion remains low over all blend times studied, while above 100% coverage, cohesion again drops rapidly. This behaviour is reasonable. If there is barely enough additive, then good surface coverage requires perfect dispersion; if there is sufficient additive a poor dispersion is tolerable. Above the required loading, excess additive will be loose, not on the

toner surface. This impedes flow until the loose additive is blended in (R812 silica alone, without toner, has a cohesion of 60%!!).

Figure 10 shows the cohesion, measured at the optimal blend time, for each surface coverage (from Figure 9). This optimal cohesion is independent of coverage, from 50% to 250%. Only at 25% coverage is cohesion higher. Thus, while it takes longer to blend at 50% or 250% theoretical coverage, equivalent flow to 100% coverage is ultimately obtained. A second toner (blend optimization not shown) does show reduced cohesion between 50% and 100% coverage. While it is not clear why the toners behave differently, in both cases near 100% coverage, based on eq 3, does indeed give optimal flow.

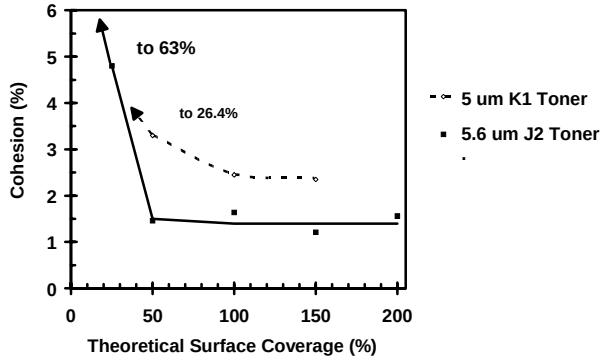

Figure 10. Optimal cohesion with additive coverage.

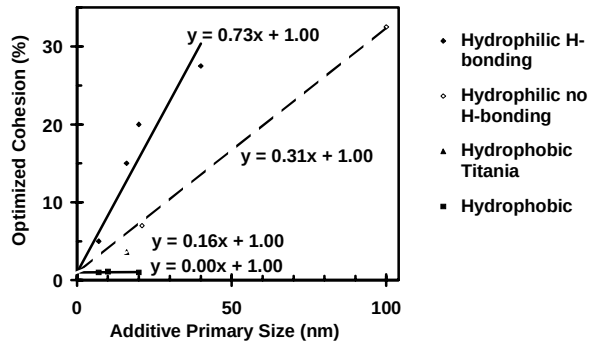

Figure 11. Cohesion with additive size and type (Toner J2)

Figure 11 shows the optimal cohesion (blending data not shown) at 100% oxide coverage, grouped according to oxide properties. Hydrophilic additives capable of H-bonding (untreated oxides with surface OH groups that form strong H-bonds) have the largest interparticle forces, due to the H-bond, Van der Waals and capillary forces. Cohesion increases linearly with the additive primary radius, as expected from eq's 4, 5 and 7. Lower cohesion arises with hydrophilic additives that do not form strong H-bonds. These additives also show the expected linear increase in cohesion with additive primary size (eq 4 and 5), but with reduced size dependence (by a factor of 2.5) due to the lack of H-bonds. The lowest cohesion is obtained with hydrophobic oxides. These are silicas treated to render them hydrophobic, removing any OH groups that might form H-bonds.[1] The cohesion with these additives is so good that the lower test limit is exceeded. To extend the test, less vibration amplitude is needed.

Figure 12 shows the effect of reduced vibration on hydrophobic additives. As the vibration decreases from the standard 1 mm vibration, cohesion increases rapidly. Figure 12 shows that cohesion does increase linearly with additive size, as expected for Van der Waals' forces (eq 3).

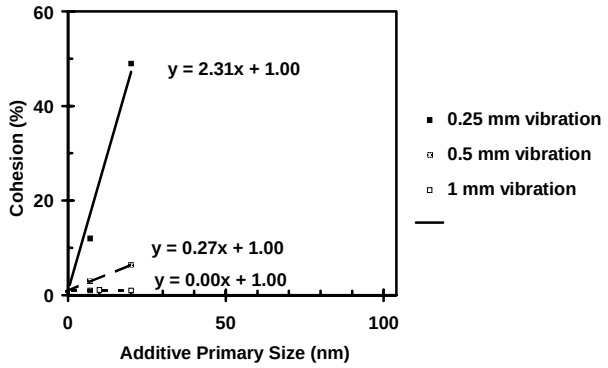

Figure 12. Cohesion with hydrophobic additives.

Conclusions

Toner flow with surface additives depends on Van der Waals, capillary, and hydrogen bonding forces, and is determined by the nano-geometry of contact. Cohesion decreases with increasing hydrophobicity, decreasing hydrogen bonding, and decreasing size.

References

1. A. Stubbe, *Proceedings of IS&T 7th International Congress on Advances in Non-Impact Printing Technologies*, 240 (1991).
2. A. R. Gutierrez, H. T. Nguyen, A. F. Diaz, *Proceedings of IS&T 8th International Congress on Advances in Non-Impact Printing Technologies*, 122 (1992).
3. R. P. N. Veregin, C. P. Tripp, M. N. V. McDougall, *Proceedings of IS&T 10th International Congress on Advances in Non-Impact Printing Technologies*, 131 (1994).
4. C. P. Tripp, R. P. N. Veregin, M. N. V. McDougall, and D. Osmond, *Langmuir*, **11**, 1858 (1995).
5. R. P. N. Veregin, C. P. Tripp, M. N. V. McDougall, and D. Osmond, *JIST*, **39**, 429 (1995).
6. H. Akagi, *Proceedings of IS&T/SPIE Color Hard Copy and Graphics Arts Symposium*, **138**,1670, (1992).
7. R. L. Carr, *Chemical Engineering*, Jan 18 and Feb 21, (1965).

8. C. P. Tripp, R. P. N. Veregin, D. Osmond, unpublished IR data.
9. N. Pilpel, *Manufacturing Chemist and Aerosol News*, **41**, 19 (1970).
10. J. N. Israelachvili, Intermolecular and Surface Forces, Academic Press, London (1985).
11. M. Chikazawa, T. Yamaguchi, T. Kanazawa, *Proc. Int. Symp. Powder Technol*., Kyoto, 202 (1981).
12. T. Kohler, H. Schubert,. *Part. Syst. Charact.,* **8**, 101 (1991).
13. M. C. Coelho, N. Harnby, *Powder Technology*, **20**, 201 (1978).

Biography

Dr. Veregin has an M.Sc. and Ph.D. in Chemistry, joining the Xerox Research Centre of Canada 13 years ago. His interests include xerographic physics, surfaces, ESR, and polymerization kinetics. He has authored 48 papers, is an inventor on 29 US patents, and is a recipient of the A. K. Doolittle Award from the American Chemical Society.